Am J Cancer Res 2024;14(2):545-561
www.ajcr.us /ISSN:2156-6976/ajcr0142170

Original Article

Autophagy-related long non-coding RNAs act as prognostic biomarkers and associate with tumor microenvironment in prostate cancer

Lu-Yao Li[1,2], Hao Zi[1,2,3], Tong Deng[1], Bing-Hui Li[1,3], Xing-Pei Guo[1,2], Dao-Jing Ming[1,2], Jin-Hui Zhang[1,2], Shuai Yuan[1], Hong Weng[1,3]

[1]Center for Evidence-Based and Translational Medicine, Zhongnan Hospital of Wuhan University, Wuhan, Hubei, China; [2]Institutes of Evidence-Based Medicine and Knowledge Translation, Henan University, Kaifeng, Henan, China; [3]Department of Urology, Institute of Urology, Zhongnan Hospital of Wuhan University, Wuhan, Hubei, China

Received February 5, 2022; Accepted November 27, 2022; Epub February 15, 2024; Published February 28, 2024

Abstract: Aberrant autophagy could promote cancer cells to survive and proliferate in prostate cancer (PCa). LncRNAs play key roles in autophagy regulatory network. We established a prognostic model, which autophagy-related lncRNAs (au-lncRNAs) were used as biomarkers to predict prognosis of individuals with PCa. Depending on au-lncRNAs from the Cancer Genome Atlas and the Human Autophagy Database, a risk score model was created. To evaluate the prediction accuracy, the calibration, Kaplan-Meier, and receiver operating characteristic curves were used. To clarify the biological function, gene set enrichment analyses (GSEA) were performed. Quantitative real-time PCR (qRT-PCR) was employed to determine the au-lncRNAs expression in PCa cell lines and healthy prostate cells for further confirmation. We identified five au-lncRNAs with prognostic significance (AC068580.6, AF131215.2, LINC00996, LINC01125 and LINC01547). The development of a risk scoring model required the utilization of multivariate Cox analysis. According to the model, we categorized PCa individuals into low- and high-risk cohorts. PCa subjects in the high-risk group had a worse disease-free survival rate than those in the low-risk group. The 1-, 3-, and 5-year periods had corresponding areas under curves (AUC) of 0.788, 0.794, and 0.818. The prognosis of individuals with PCa could be predicted by the model with accuracy. Further analysis with GSEA showed that the prognostic model was associated with the tumor microenvironment, including immunotherapy, cancer-related inflammation, and metabolic reprogramming. Four lncRNAs expression in PCa cell lines was greater than that in healthy prostate cells. The au-lncRNA prognostic model has significant clinical implications in prognosis of PCa patient.

Keywords: Long non-coding RNA, autophagy, bioinformatics, biomarkers, tumor microenvironment, prostate cancer, prognostic model

Introduction

Prostate cancer (PCa) has a worldwide standardized incidence rate of 37.86/100,000 in 2017 and a standardized death rate of 13.11/100,000. Compared with 1990, the global standardized incidence rate increased by 24.17%, and the standardized mortality rate decreased by 13.69% [1]. Although the mortality rate of PCa has declined globally, there are still many countries where PCa is the primary reason of malignancy death among men [2]. Currently, Prostate-specific antigen (PSA) levels and pathological stages are the main monitoring indicators for PCa. Although extensive research has been conducted on the mechanism of carcinogenesis, the cause of PCa is still unclear. Therefore, it is extremely important to create a prognostic prediction model for PCa patients in order to improve their treatment outcomes.

Investigations on the possibility of long non-coding RNAs (lncRNAs) in people with cancer are continually expanding owing to their raised specificity and simplicity of recognition in tissues, serum, urine, and other specimens. LncRNAs have a role in protein-protein, protein-DNA, and protein-RNA interactions in addition to chromatin remodeling, miRNA control, and

https://doi.org/10.62347/XTDZ5687

gene transcription regulation [3]. There are more and more evidences show that lncRNAs are in-volved in a variety of biological mechanisms, like tumor growth, differentiation, death, drug resistance, metastasis and TME, indicating that targeting lncRNAs may be useful for the identification and therapy of tumor cases, including PCa [3-7]. In recent years, hundreds of lncRNAs related to PCa have been recognized through transcriptomic comparative analysis of PCa and benign tissues [8, 9]. For instance, up-regulation of lncRNA PCAT1 may cause up-regulation of androgen response genes, including androgen receptor and lysine-specific histone demethylase 1A (LSD1), which would assist in the development of PCa [10]. Researchers believe that lncRNAs have a great deal of potential usefulness as novel markers and clinical treatment targets for PCa because of the specificity and functional significance of lncRNAs expression [11].

Investigations have revealed that lncRNAs have crucial functions in the complex autophagy regulatory network by regulating a range of autophagy-related DNA, RNA or proteins [12]. Autophagy is related to the etiology of cancer and acts as a death or survival fac-tor under different circumstances. Autophagy defects may promote cancer transformation of healthy cells, and enhanced autophagy response may also enable cancer cells to survive and proliferate under unfavorable microenvironmental conditions [13]. In opinion of the function of autophagy in cancer progression, autophagy inhibition may be a strategy for cancer treatment [14]. In PCa, the inhibition of autophagy can in-crease the sensitivity of cells to docetaxel management [15]. A study also found that in the treatment of PCa, docetaxel inhibits the expression of KLF5 and promotes cell autophagy, causing desensitization to the drug and cell survival in castration-resistant PCa cells [16]. The lncRNAs associated with autophagy may provide new options of diagnosis, treatment and prognosis options for PCa patients. To determine cases who can advantage from autophagy-based therapy, predictive markers for autophagy drug treatment response are necessary.

Tumor microenvironment (TME) has always been a hotspot in PCa research, which is associated with tumor occurrence, growth, and metastasis. Through nutrient-generating autophagy, transformed cells engage surrounding normal cells as important contributors to early tumor growth [17]. Study have shown that that autophagy, immunobiology and response to treatment were correlated with hormone-dependent malignancy development and progression [18]. Ma et al thought that suppression of autophagy by its suppressor benefits the therapy of abiraterone for castration resistance prostate cancer (CRPC) patients [19]. In LNCaP cells, androgen deprivation triggered autophagy and lipophagy, resulting in LD breakdown and cell survival [20].

In this investigation, by using the lncRNAs information of PCa patients in the Cancer Genome Atlas (TCGA) database and the Human Autophagy Database (HADb), we identified autophagy-related lncRNA (au-lncRNA) connected to the prognosis of PCa, and constructed a PCa au-lncRNA prognostic model that could be employed as a prognostic predictor for PCa. The expression of lncRNAs were also verified in prostate cell lines. The results of this study provide novel concepts and directions for further investigation on the pathogenesis and prognosis of PCa.

Materials and methods

Data source and processing

TCGA-PRAD expression data and clinical information tables have been down-loaded from TCGA database (https://cancergenome.nih.gov/) through Xena. The data of 481 cases of primary cancer samples and 51 cases of normal control samples were extracted. 232 autophagy-related genes were acquired in HADb (http://www.autophagy.lu/index.html).

Identification of au-lncRNA

The gencode.v22.annotation.gtf annotation file was downloaded from the TCGA official website, and 14,826 lncRNA genes were extracted from the file using the R package “rtracklayer”. Pearson correlation analysis was performed on the autophagy gene and lncRNA gene of primary cancer (01A) samples through the cor and cor.test() functions of the R software. A lncRNA was deemed to be an au-lncRNA if its absolute correlation co-efficient was higher than 0.7 ($|R| > 0.7$) and its *P* value was less than 0.05 ($P < 0.05$).

Identification of differentially expressed au-lncRNAs

An analysis of au-lncRNA differential expression was performed employing the R package "DESeq2" on the sample data of normal and cancer patients, and the *P* values adj.*p* value < 0.05 and |log2FC| > 1 corrected by Benjamini-Hochberg (FDR) were used as the screening threshold to obtain the differentially expressed au-lncRNA (DE-au-lncRNA). The volcano map was drawn utilizing the R package "ggpubr", and the DE-au-lncRNA heat map was created employing R package "ComplexHeatmap".

Establish a prognostic model of au-lncRNA

According to the patient's survival time and status, the Coxph function of the R software package "survival" was employed to assess the relation between au-lncRNA expression and prognosis through univariate Cox regression analysis. Significant difference is defined as P < 0.05. The forest plots of all genes with univariate Cox factor P < 0.05 were drawn using the R package "forestplot". Using the results of a univariate Cox regression study, a LASSO regression was conducted using the R package "glmnet". The prognosis-related au-lncRNA was determined employing LASSO regression analysis. Using the Coxph function of the R package, a multi-factor Cox regression model was constructed according to survival time and status, and au-lncRNA was screened according to the *p* value. According to survival time and status, the survival curve of each characteristic prognostic au-lncRNA was drawn by the R software packages "Survminer" and "Survival". Depending on the median gene expression level, a high and reduced cohort of patients was divided to show the prognostic difference between each group. The key factors were screened out through the au-lncRNAs interaction network (|R| > 0.7, P < 0.05), and visualized with cytoscape software. The R package "ggalluvial" draws the Sankey diagram. Then, each patient's risk score was estimated. Subjects with PCa were split into low- and high-risk groups based on their median risk scores.

Prognostic performance evaluation of risk scoring model and validation of external data sets

In order to establish an effective prognostic prediction model, 70% of the TCGA samples were used as modeling group, and 30% of the samples were used as the confirmation set. The R packages "Survminer" and "Survival" are employed to construct the survival curves of the high-risk and low-risk cohorts, respectively. The ROC curve is drawn using the R package "SurvivalROC", which can produce 1-year, 3-year, and 5-year ROC curves in addition to AUC. The range of AUC values is 0.5 to 1.0. AUC > 0.9 indicates elevated accuracy, AUC 0.5-0.7 indicates poor accuracy, AUC 0.7-0.9 indicates medium accuracy, and AUC 0.5 indicates no predictive ability. The survival scatter plots were created employing the R package "ggplot2", and the heat maps were created utilizing the R package "ComplexHeatmap".

Establish and verify prognostic nomogram

According to survival time and survival status, univariate and multivariate cox regression models were constructed using the coxph function of the R package "survival". Cox univariate and multivariate forest plots were established employing the R package "forestplot". The nomogram and the consistency curve were drawn using the R pack-age "rms".

Gene set enrichment analysis (GSEA)

The variations between the high- and low-risk cohorts were examined utilizing R package DESeq2, the GSEA gene ontology (GO) and Kyoto Encyclopedia of Genes and Genomes (KEGG) enrichment analysis was conducted using the R package "clusterProfiler", and the top 5 enrichment results were displayed using the R package "enrichplot".

Cell culture

The Cell Bank of the Chinese Academy of Sciences in China was employed to obtain PCa cells (22RV-1, PC-3, DU145, LNCaP), in addition to healthy prostate cells (WPMY-1). RPMI-1640 medium (Solarbio, Beijing, China), treated with 10% fetal bovine serum (FBS; Gibco, Shanghai, China), and 1% antibiotic combination (penicillin and streptomycin), was employed to incubate WPMY-1, 22RV-1, PC-3, and LNCaP cells. 10% fetal bovine serum was added to Dulbecco's modified Eagle's medium (DMEM; Invitrogen, Shanghai, China) for the cultivation of DU145 cells (FBS; Gibco, Shanghai, China). Cells were preserved at 37°C in a humid incubator that had 5% CO_2 added to it.

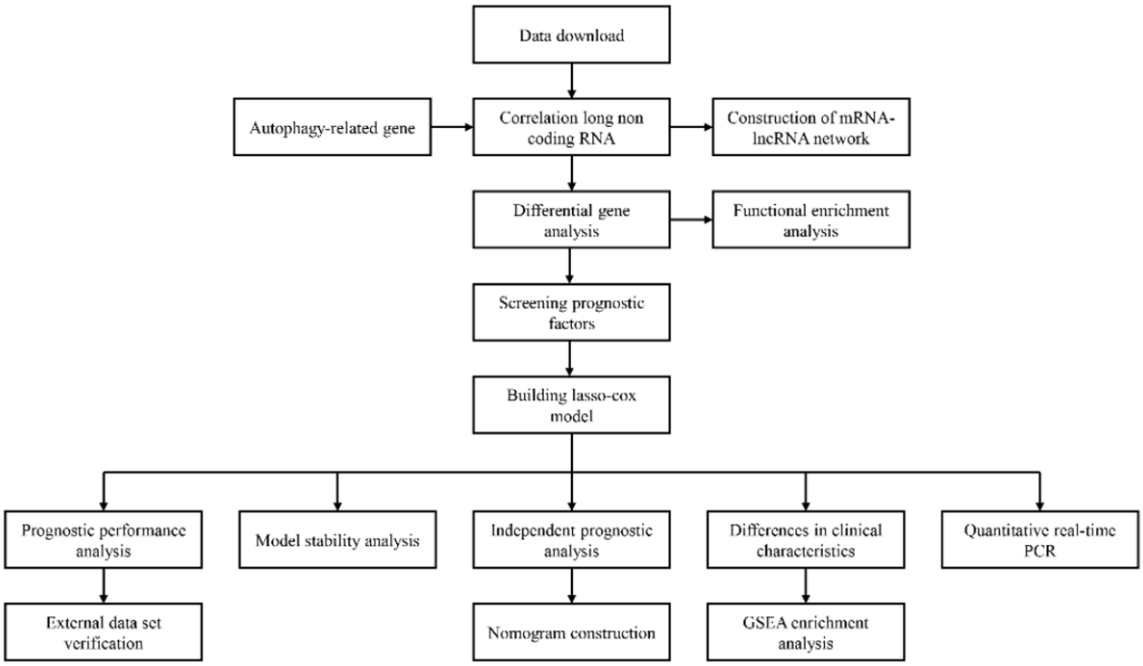

Figure 1. Flowchart for identification and validation of an autophagy-related lncRNA signature in prostate cancer patients.

Quantitative real-time PCR

Utilizing RNA extraction kit (Eastep®Super Total RNA ex-traction kit), total RNA was extracted. The purity and quantity of RNA were determined using a NanoDrop 2000 spectrophotometer from Thermo Fisher Scientific. Every total RNA was reverse transcribed into cDNA for qRT-PCR analysis utilizing TaKaRa SYBR Premix ExTaq kit. SYBR Green (TaKaRa) was employed for QRT-PCR, and the information was assessed using the CFX Connect real-time system (BIO-RAD, California, USA). The following were the thermocycling conditions: following 40 cycles of 95°C for 5 sec and 60°C for 30 sec, 95°C for 10 sec. GAPDH was employed to normalize RNA expression. The technique of ΔCt was applied to evaluate the data. The experiment was repeated at least three times. Table S1 lists five primers for au-lncRNA.

Results

Identification of au-lncRNAs and differentially expressed au-lncRNAs

According to the TCGA database, 14826 long noncoding RNAs were identified in PCa patients. Typically, 232 genes connected to autophagy were also recognized from the HADb. The analysis process was presented in **Figure 1**. Pearson correlation analysis between these lncRNAs and autophagy-related genes was conducted, which identified 419 au-lncRNAs, the Representative correlation plots were shown in Figure S1. Among these au-lncRNAs, 114 lncRNAs were differentially expressed, of which 91 au-lncRNAs were raised and 23 au-lncRNAs were reduced (**Figure 2A**, **2B**).

Creation and validation of a prostate cancer prognostic risk-related au-lncRNA signature model

We screened the prognostic value of the 114 differentially expressed au-lncRNAs by univariate Cox regression analysis and constructed a forest plot using 21 prognostic related au-lncRNAs, including 2 low-risk lncRNAs and 19 high-risk lncRNAs (**Figure 3A**). Subsequently, in the modeling cohort, the 21 prognostic-related au-lncRNA were used for Lasso regression analysis and multiple Cox proportional hazard regression analysis, and 5 lncRNAs were recognized with significant values of prognosis (AC068580.6, AF131215.2, LINC00996, LINC01125 and LINC01547) (**Figure 3B-D**). We also established a visual co-expression network of

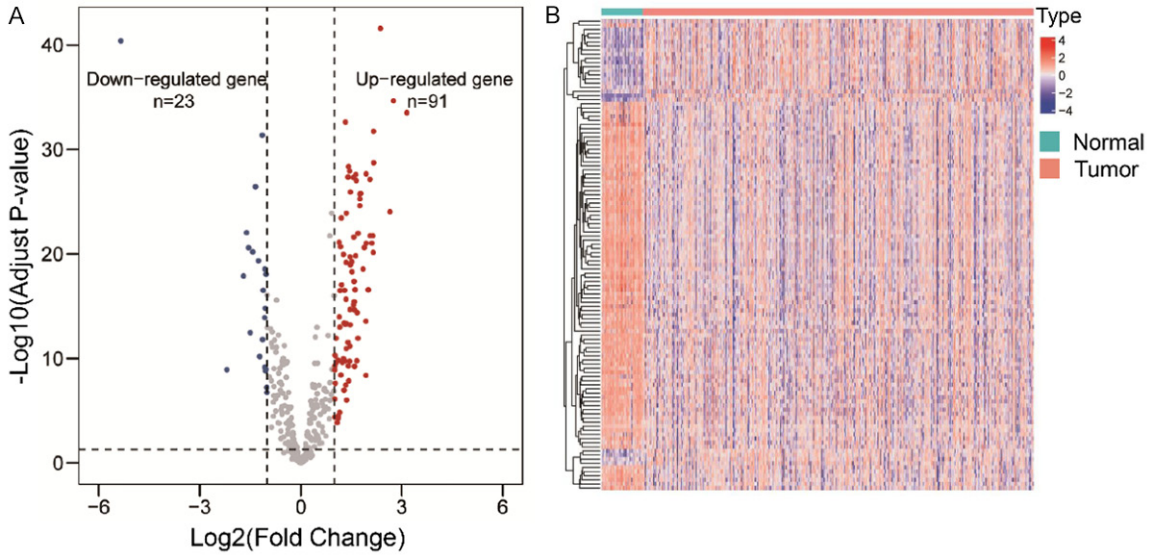

Figure 2. Difference analysis of au-lncRNAs. A. Volcano plots of the distributions of 419 au-lncRNAs (the red dots indicate up-regulated au-lncRNAs and the blue dots indicate the down-regulated au-lncRNAs, while gray dots indicate no difference). B. Heatmap of the expression profiles of 114 differentially expressed lncRNAs in prostate cancer and normal tissues.

5 au-lncRNAs-mRNAs with prognostic value (**Figure 3E**, **3F**). Lastly, the following formula was employed to create a model for 5 au-lncRNA predictive risk score: risk score = (0.502 × expression level of AC068580.6) + (-0.447 × expression level of AF131215.2) + (0.280 × expression level of LINC00996) + (0.411 × LINC01125 expression level) + (-0.476 × LINC01547 expression level). In addition, we found that AC068580.6, LINC00996 and LINC01125 were risk factors with HR > 1, while AF131215.2 and LINC01547 were protective factors with HR < 1. In the Kaplan-Meier survival curve analysis of five au-lncRNAs. AC068580.6, LINC00996 and LINC01125 overexpression were associated with poor prognosis, and high expression of AF131215.2 and LINC01547 were associated with good prognosis (Figure S2A-E).

Individuals in the modeling group were divided into high-risk (n = 157) and low-risk (n = 157) cohorts depended on their median risk scores. In Kaplan-Meier survival curve, cases with high-risk scores had substantially shorter disease-free survival (DFS) times than those with low-risk levels (**Figure 4A**).

To assess the predictive value of the prognostic model, 1-, 3- and 5-year receiver operator characteristic (ROC) curves were drawn. The zone below curve (AUC) values were 0.788 (1-year ROC), 0.794 (3-year ROC) and 0.818 (5-year ROC) (**Figure 4B**). Patients with greater risk scores have a shorter DFS time than those with lesser risk scores (**Figure 4C**). In addition, the heat map exhibited that the five au-lncRNAs were substantially differently expressed in high-risk cohort and low-risk cohort (**Figure 4D**). Risk factors were higher in the high-risk group (LINC00996, AC068580.6 and LINC01125), in contrast, the low-risk cohort expressed greater levels of protective factors (AF131215.2, LINC01547). These findings showed that our model could predict PCa patients' prognoses with a reasonable degree of accuracy.

We examine the prognostic efficacy in the validation dataset employing the same method to further evaluate the prognostic value of the 5 au-lncRNAs panel. Individuals with high-risk ratings had shorter DFS times than individuals with low-risk scores, according to Kaplan-Meier survival curves (Figure S3A). One-, three-, and five-year survival rates' AUC values were 0.738, 0.802, and 0.805, respectively (Figure S3B). The DFS time is shorter for individuals with higher risk ratings than it is for those with reduced risk scores (Figure S3C). Five au-lncRNAs showed a substantial difference in expression between the high- and the reduced risk group (Figure S3D). In conclusion, the prognostic model of au-lncRNAs had the capability to expect the survival of individuals with PCa.

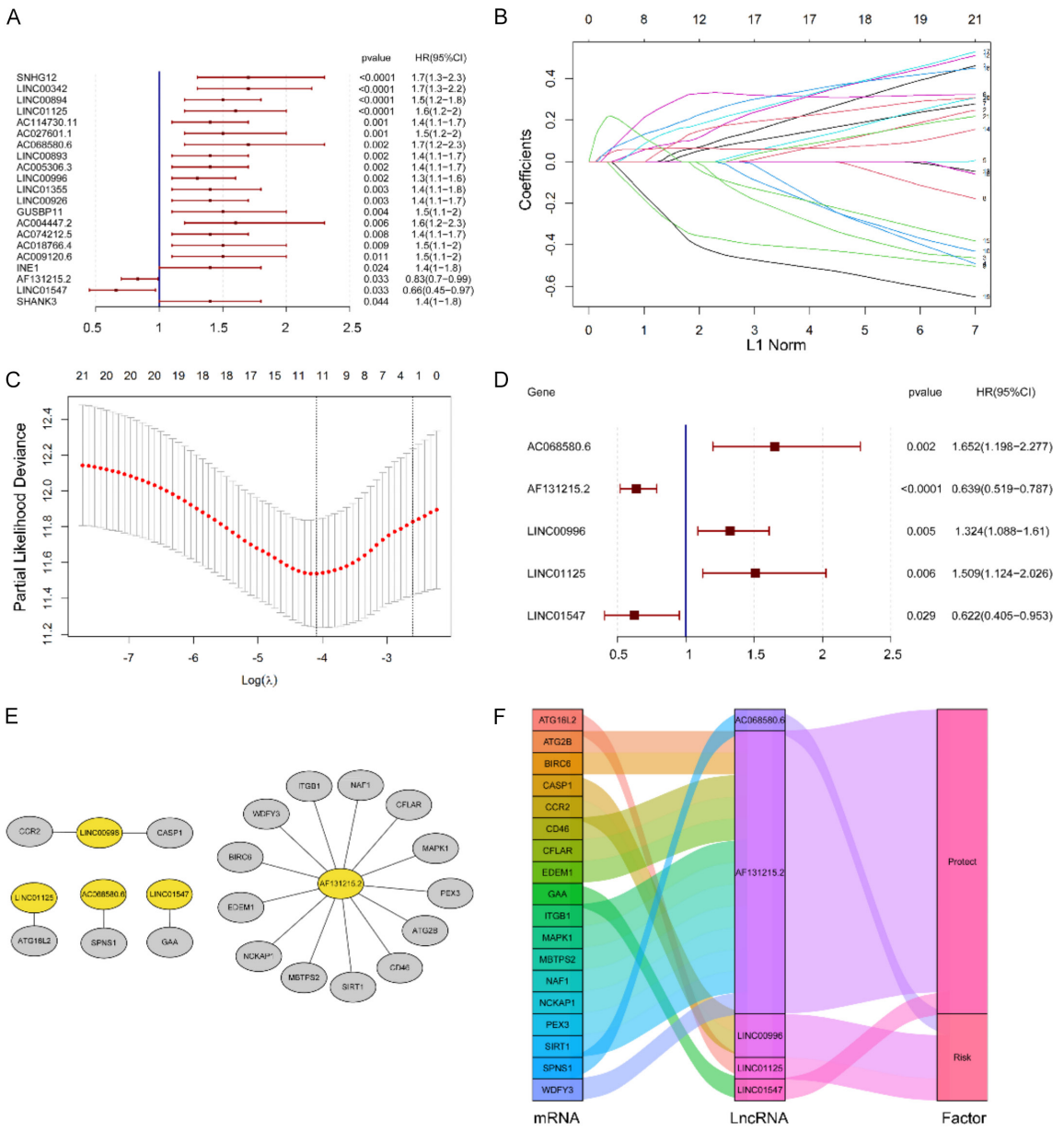

Figure 3. Identify au-lncRNAs with autophagy value. A. Forest plot depicting associations between au-lncRNAs and risk value determined via univariate Cox regression analysis. B. LASSO coefficient profiles of genes associated with overall survival of PCa. C. Partial likelihood deviance was plotted versus log (λ). The vertical dotted line indicates the lambda value with the minimum error and the largest lambda value, where the deviance is within one standard error of the mini-mum. D. Forest plot depicting associations between lncRNAs and risk value determined via multivariate Cox regression analysis. E. Autophagy-related lncRNA-mRNA network diagram. The yellow circle corresponds to lncRNA related to autophagy, and the gray circle corresponds to mRNA. F. Mulberry diagram, showing the degree of connection (risk/protective) between 18 mRNAs and 5 lncRNAs related to autophagy.

Establishment and evaluation of the prostate cancer au-lncRNA prognostic model

We used univariate and multivariate Cox regression analysis to determine if the risk model of au-lncRNA is a reliable predictor of PCa prognosis. The findings demonstrated that PSA, Gleason, T, N, and recurrence were substantially correlated with patient survival status and predictive survival time based on the risk score of au-lncRNAs (**Figure 5A**). Furthermore, multivariate Cox regression analysis shown that risk score, TP53, T phases, and recurrence are each independent prognostic markers for the length of survival and survival status of Patients with PCa (**Figure 5B**).

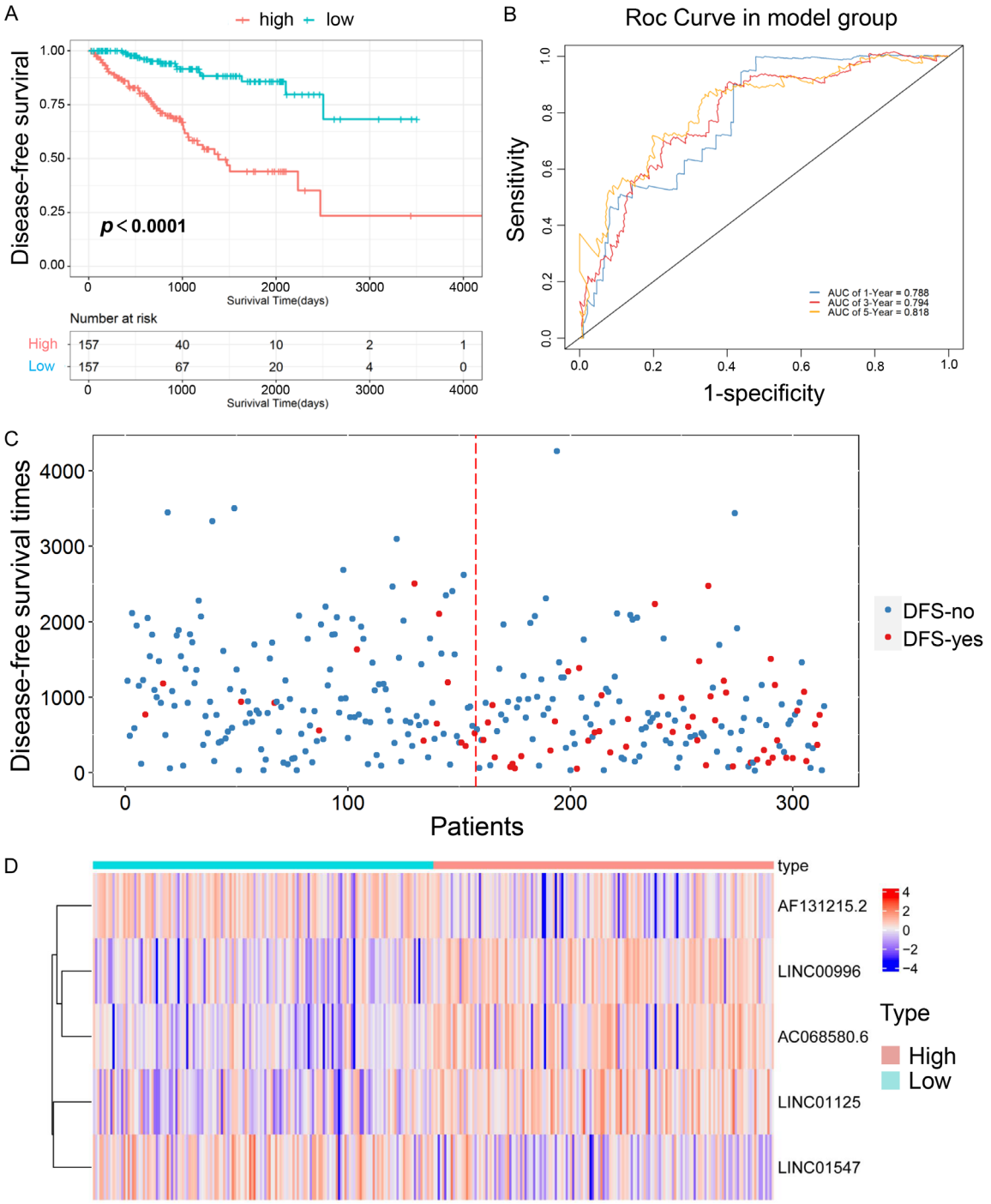

Figure 4. Construction and evaluation of prognostic model of au-lncRNAs in PCa patients. A. Kaplan-Meier survival curves of the high-risk group and the low-risk group. B. ROC curve based on risk scoring model. C. Scatter plot of the survival situation of the high-risk group and the low-risk group. D. The expression heat map of five autophagy-related lncRNAs.

Depending on the signature model of au-lncRNAs combined with the above-mentioned clinicopathological characteristics, we constructed a nomogram (**Figure 5C**). A vertical line can be drawn between the total point axis and each prognostic axis to calculate the survival rate of individuals with PCa at 1, 3 and 5 years. The calibration curve displays the consistency between the anticipated and actual survival rates (**Figure 5D-F**).

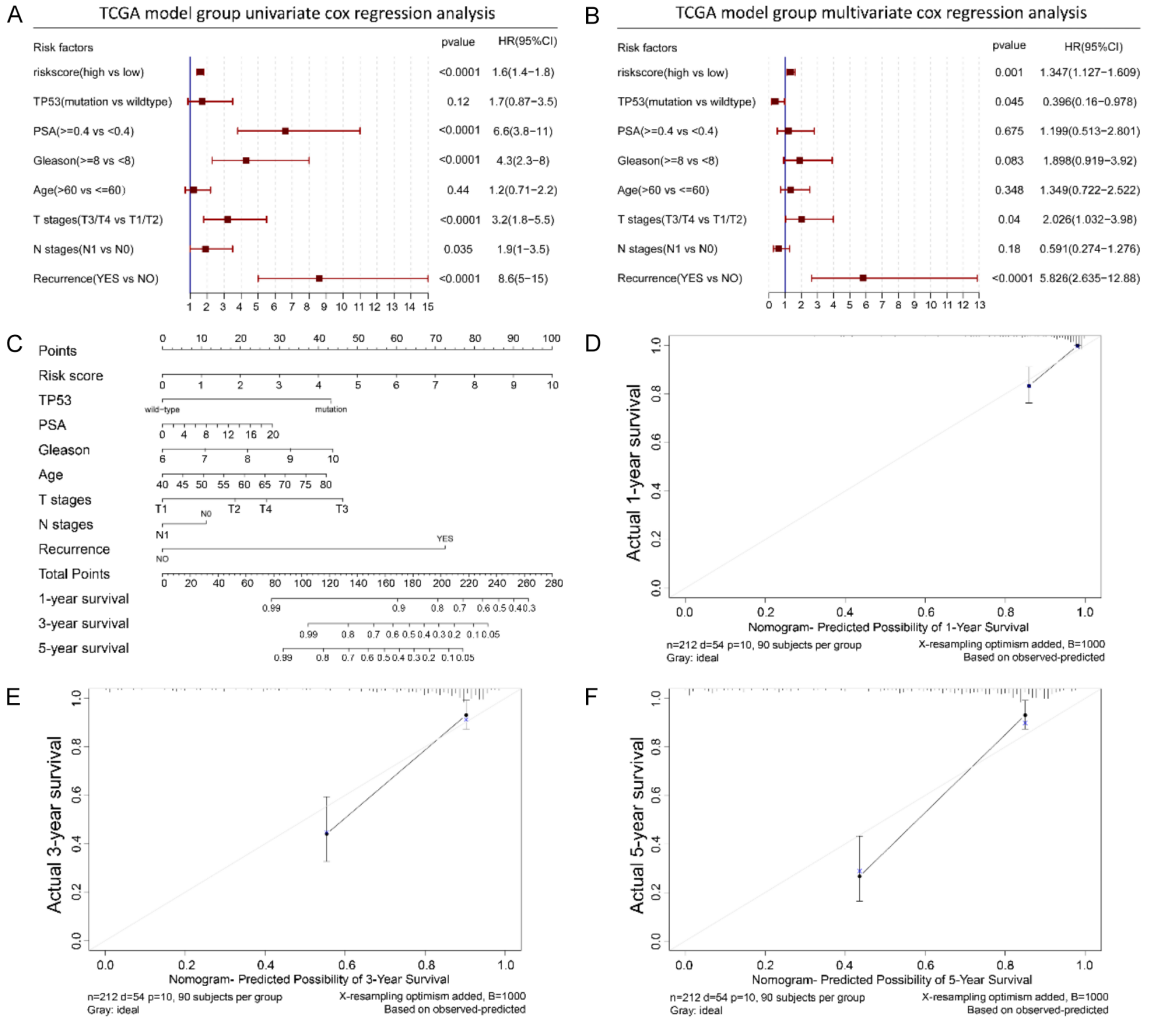

Figure 5. Construction and verification of au-lncRNA prognostic nomogram. A. Univariate Cox regression results. B. Multivariate Cox analysis results. C. A prognostic nomogram constructed based on the prognostic risk scores of autophagy-related lncRNA and clinicopathological parameters such as TP53, PSA, Gleason score, age, T stage, N stage, recurrence, etc., can predict 1, 3, and 3 of prostate cancer patients 5-year survival rate. D-F. Concordance curves between the predict-ed and observed values of 1-year, 3-year, and 5-year survival rates for high-risk and low-risk prostate cancer patients.

Clinicopathological characteristics and potential biological functions of au-lncRNAs signature model

We next explored the relationship between Au-lncRNAs signature model and clinicopathological characteristics (**Figure 6A**). The outcomes revealed that the risk score of Au-lncRNAs signature model was higher in TP53 mutant patients than in TP53 wild-type, though the alteration was not substantially significant (P = 0.085) (**Figure 6B**). Moreover, the risk score was significant higher in PSA ≥ 4.0 (P = 0.0013) (**Figure 6C**), Gleason ≥ 8 (P < 0.0001) (**Figure 6D**), age > 60 (P = 0.023) (**Figure 6E**), advanced T stages (T3/T4) (P = 0.041) (**Figure 6F**), N1 stage (P = 0.005) (**Figure 6G**) and recurrence (P = 0.0045) (**Figure 6H**) patients. Figure S4 showed the prediction of DFS time in different clinical subgroups by the prognostic model of au-lncRNAs, which indicated that most subgroups were significantly associated with patient prognosis. These results indicate that Au-lncRNAs signature model could be correlated with malignant progression of PCa.

To investigate these au-lncRNAs' potential biological function. On the differentially expressed au-lncRNAs between the high- and the low-risk group, we also conducted GO enrichment anal-

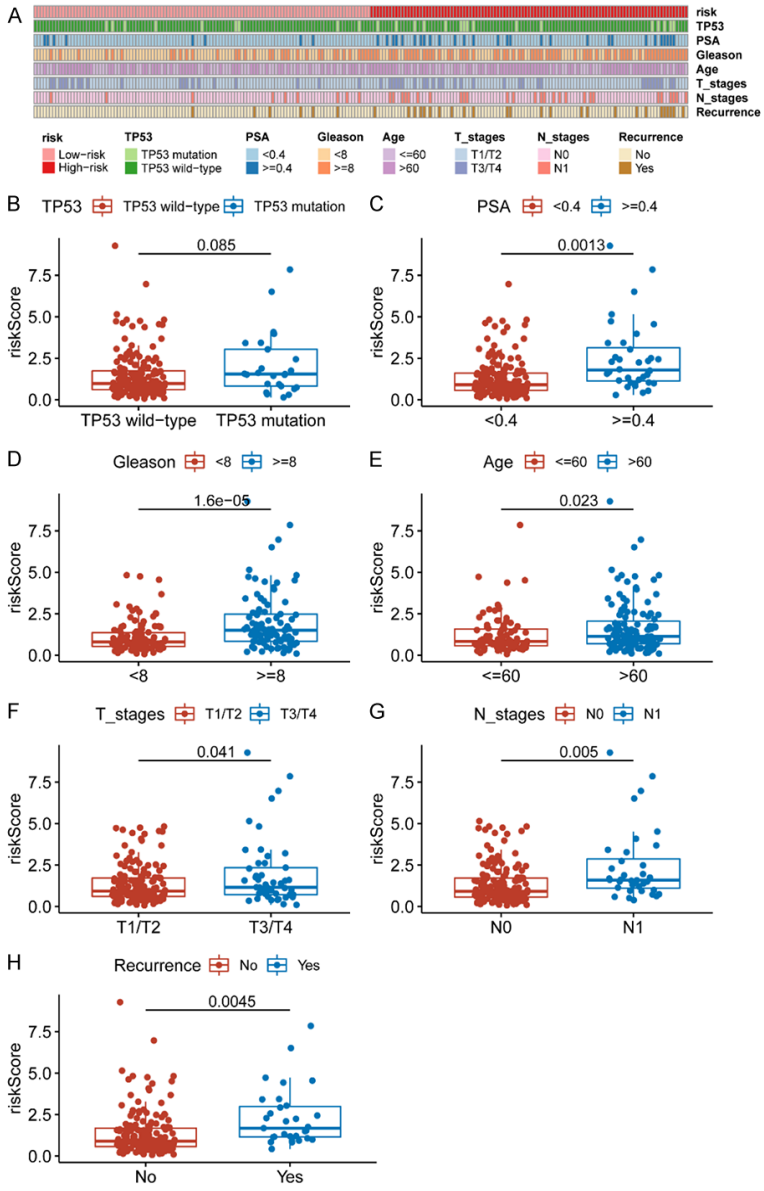

Figure 6. Correlation analysis between the risk score of the au-lncRNAs prognostic model and the different clinicopathological characteristics of PCa patients. A. Heat map between the high and low risk score group and the different clinicopathological characteristics of PCa patients. B. TP53 (mutant and wild type). C. PSA (< 4.0 ng/ml and ≥ 4.0 ng/ml). D. Gleason score (< 8 and ≥ 8). E. Age (≤ 60 and > 60). F. T grades (T1/T2 and T3/T4). G. N grades (N0 and N1). H. Recurrence (yes and no).

ysis and KEGG mechanism analysis, and we displayed the top 5 enrichment outcomes. GO_BP enrichment examination exhibited that these genes were enriched in Cdc42 protein signal transduction, chylomicron assembly, negative regulation of IL-1β secretion, positive regulation of IL-2 biosynthesis and circulating immunoglobulin-mediated humoral immune response regulation (**Figure 7A**). GO_CC enrichment assessment exhibited that these genes were enriched in banded collagen fibrils, chylomicrons, fibrous collagen trimers, hemoglobin complexes and T cell receptor complexes (**Figure 7B**). These genes were enriched in haptoglobin binding, IL-1 receptor binding, lipopeptide binding, pattern recognition receptor activity, and triglyceride lipase activity, according to GO MF enrichment analysis (**Figure 7C**). These genes are involved in the mechanisms for primary immunodeficiency, allograft rejection, asthma, intestinal immune network for IgA synthesis, viral protein interaction with cytokines and cytokine receptors, and other mechanisms, according to the KEGG pathway assessment (**Figure 7D**).

Validation the expression of 5 au-lncRNAs in prostate cancer cells

The five au-lncRNAs in PCa cell lines were studied using the qRT-PCR method. In this investigation, four PCa cell lines-22RV-1, PC-3, DU145, and LNCaP-were employed. The five lncRNAs' expression in cell lines was verified using the value of ΔCt. A lower level of lncRNA expression corresponds to a greater value of ΔCt. According to the findings, LINC00996 and AF131215 were strongly expressed in PCa, as were LINC01125 and LINC01547.2 were poor (**Figure 8A**). **Figure 8B** illustrates the mean value of ΔCt of each au-lncRNAs in all cell lines: LINC01125 = 9.51, LINC00996 = 14.37, AC068580.6 = 12.215, LINC01547 = 10.8775 and AF131215.2 = 14.3675. The qRT-PCR results also showed that compared with normal prostate cells (WPMY-1), the expression of LINC01125, LINC01547, LINC00996 and

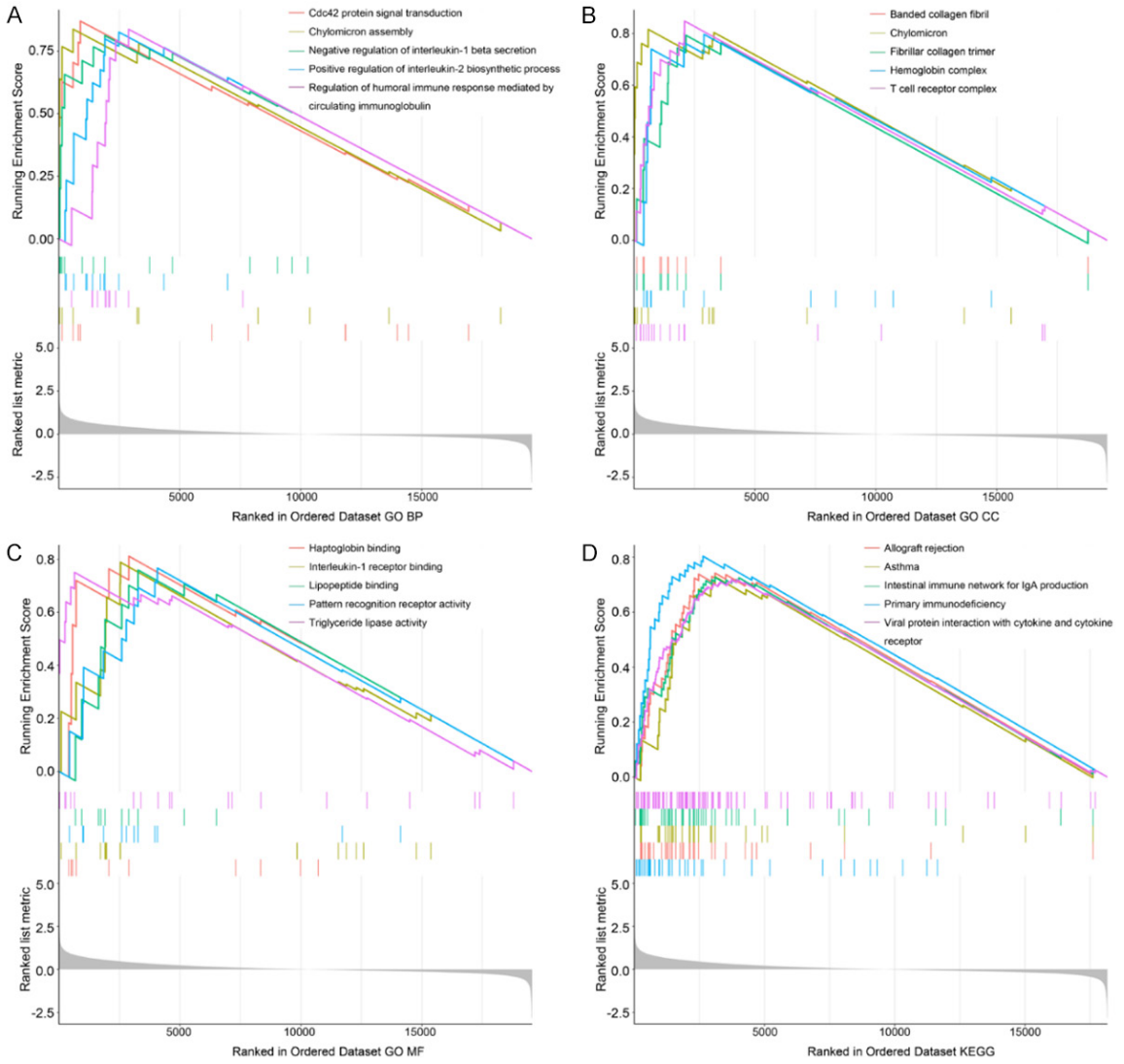

Figure 7. Gene set enrichment analysis of high-risk and low-risk prostate cancer patients based on the prognostic model of au-lncRNAs (GSEA, left is High risk, right is Low risk). A. GO_BP enrichment analysis. B. GO_CC enrichment analysis. C. GO_MF enrichment analysis. D. KEGG pathway analysis.

AF131215.2 in the PCa cell line was significantly increased, while the expression of AC068580.6 had no difference (**Figure 8C-G**).

Discussion

PCa, a typical malignant cancer of the urinary tract, is second in frequency among cancer-related deaths in Western developed nations [21]. After initial treatment, the recurrence rate of PCa varies with stage, Gleason score, and PSA level [22]. Though 20% to 30% of individuals with medically limited disease will deteriorate within 5 years after first treatment [23], anticipating the risk of recurrence or metastatic development in subjects are still challenging. There are studies which have explored the correlation between autophagy-related genes and PCa [24, 25], but there were many differences in our study. Firstly, we employed the validation data set to verify the established model to make the prediction model more stable and reliable. Secondly, our study further found that the au-lncRNAs were associated with TME and tumor immunity, providing evidence support for research and treatment in PCa. Thirdly, to further explore the biological significance of the au-lncRNA, more importantly we verified them in PCa and normal cell lines. In this investigation, we build a signature model depending on five au-lncRNAs (AC068580.6, AF131215.2, LINC00996, LINC01125 and LINC01547). The

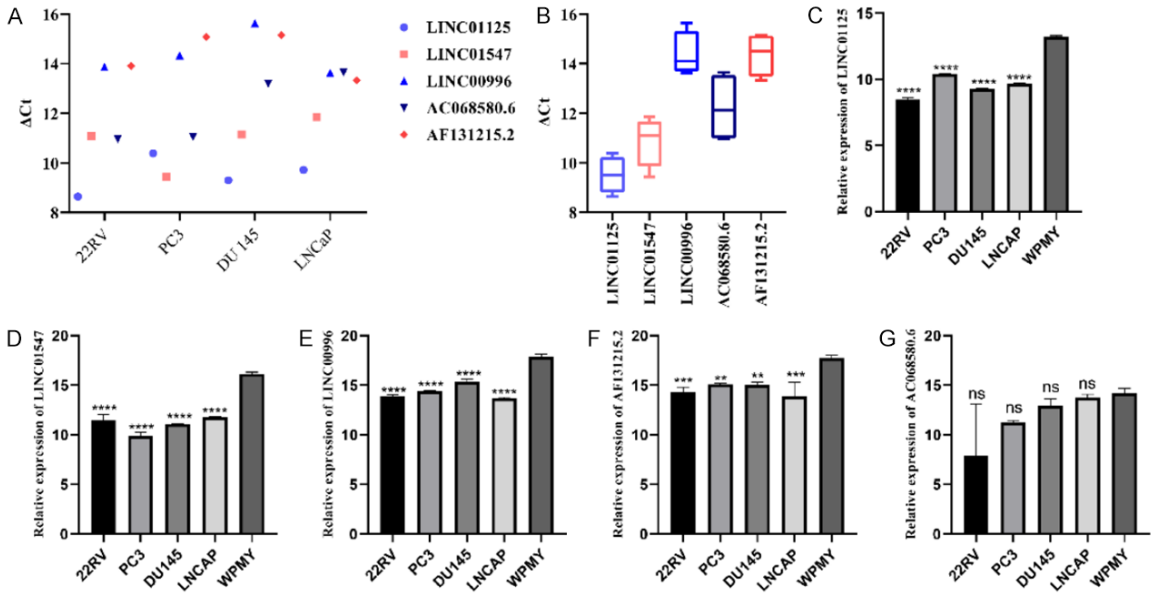

Figure 8. The expression levels of the five au-lncRNAs in PCa cell lines. A. The expression of the 5 lncRNAs in each cell lines. B. The total expression levels of the five au-lncRNAs in 4 cell lines. C-F. qRT-PCR results showed that LINC01125, LINC01547, LINC00996 and AF131215.2 expression was higher in prostate cancer cell lines than in the normal cell lines. **P < 0.01, ***P < 0.001, ****P < 0.0001. G. qRT-PCR results showed that AC068580.6 expression in prostate cancer cell lines was not different from that of normal cell lines.

1, 3, and 5-year ROC values obtained from the model evaluation in the modeling data set are 0.788, 0.794, 0.818, respectively, and the 1, 3, and 5-year ROC values obtained from the model evaluation in the validation set are 0.738, 0.802, 0.805, respectively. The model is very accurate in estimating PCa patients' DFS time. Lastly, the robustness analysis of the model, the nomogram creation, the enrichment analysis, and the qRT-PCR validation were assessed. The connection between the signature model and clinical features was also investigated. The results show that these five au-lncRNAs are strictly connected to the prognosis of PCa, and may be a powerful indicator of the clinical prognosis of individuals with PCa.

So far, among these 5 au-lncRNAs, LINC00996, LINC01125 and LINC01547 have been studied in PCa or other cancers. According to reports, the decrease of LINC00996 expression may be connected to the incidence and metastasis of colorectal cancer, and the depletion of LINC-00996 is related to the adverse outcome of colorectal cancer patients [26]. In a study on the prognostic risk model of multiple myeloma, LINC00996 is also a lncRNA that is strictly associated with the prognosis of multiple myeloma [27]. It can be seen that LINC00996 is related to prognosis in many tumors. In another study, LINC00996 was also used as a lncRNA closely related to the prognosis of head and neck cancers [28]. Studies have found that overexpression of LINC01125 can inhibit the growth of ovarian cancer and breast cancer [29, 30]. But in this study, LINC01125 is a risk factor for the prognosis of PCa. So, whether this difference is caused by our sample size or other reasons can be the focus of our next phase of research. In a study on ovarian cancer, LINC01547 as one of the genetic signatures was substantially associated with the overall survival rate of subjects with ovarian cancer [31].

GO enrichment assessment and gene KEGG mechanism analysis were performed on the differentially expressed au-lncRNAs. The results show that au-lncRNAs mainly focus on cell functions and pathways such as immunity, lipid and receptor regulation. Cdc42 is a guanine trinucleotide enzyme that can switch between an active form and an inactive form, thereby acting as a molecular "switch" to perform a variety of important regulatory functions in cell migration [32]. Studies have shown that residual lipoprotein (RLP) is a lipoprotein rich in triglycerides, which is created by the hydrolysis of

very low-density lipoprotein and chylomicrons. Growth and signal transduction of PCa cells are directly affected by RLP [33]. Many different research fields have pointed out the potential function of immunity in the occurrence of PCa and cancer growth [34]. Investigations have revealed that NK cells activated by IL-2 have the capability to kill NK cell-resistant PCa cell line PC3 [35]. IL-1β is up-regulated in PCa, and its expression is correlated with Gleason score ≥ 7 [36]. Mouse prostate epithelial-specific *Pten* gene knockout can up-regulate the genes encoding CSF1 and IL-1β, and it can also encourage the development of local myeloid-derived inhibitor cells and immunosuppression [37].

Our research suggests the Correlation of prognostic model of au-lncRNAs and TME. Gene enrichment assessment exhibited that these genes were enriched in humoral immune response regulation, IL-1 receptor binding, T cell receptor complexes, pattern recognition receptor activity and triglyceride lipase activity and primary immunodeficiency. Zhunussova et al have found that TME could influence energy metabolism by mitochondria in PCa cells [38]. Kasahara et al show that humoral immune system antibodies against tumors suppress TME through FcγRIIB signaling [39]. Multiple functions of humoral immunity are implicated in antitumor defense, like antigen processing and presentation, cytokine-mediated signaling and antibacterial defense [40]. Different types of cells are found in the TME, which promotes or inhibits the tumor through immune checkpoint blockade therapy [41]. TCR is closely associated with CAR-T-based tumor immunotherapy. The fifth-generation chimeric antigen receptors (CARs) were constructed depending on the second-generation CARs. Gene editing inhibited the ex-pression of TCR gene and promoted the ablation of TCR α chain and β chain [42]. The amount and quality of target identification are regulated by the repertoire of 'neoepitope'-specific T-cell receptors on tumor-infiltrating lymphocytes or peripheral T-cells. Targeting tumor-stromal epitopes might potentially alter the immunological environment in TME to achieve tumor containment [43]. Immune responses are elicited without infection by Pattern recognition receptors (PRRs), which regulate tumor immunity. Activating or inhibiting PRRs could lead to effective cancer immunotherapy [44]. Numerous intracellular signaling processes derive from the role of the pattern-recognition receptor, receptor for advanced glycation end-products (RAGE), which proliferate and prolong colorectal cancer. The survival of colon cancer cells and RAGE expression are closely correlated. Tumorigenesis, which elevates and develops in the stressed TME, is influenced by RAGE [45]. The capability of TLR and RLR agonists to activate both innate and adaptive immunity is a necessity for clinical success [46]. Antitumor CD8+ cytotoxic T cells are efficiently activated and strong type I interferon responses are induced by RNA-based compounds stimulating TLR7 or MDA-5 [47, 48].

Collagen is highly aligned in the extracellular matrix of the TME. The result is directional migration, which facilitates efficient migration out of the tumor [49]. Invasion of cancer cells and metastasis are significantly affected by collagen fibril maturation in the TME. Cell migration is enhanced by fiber-like tracks [50]. It has been shown that collagen fibrils assist cancer cells in aligning themselves and acquiring a best shape. The findings point to a novel function for stromal components in cancers: preserving anchorage and shape to allow cancer cells to grow [51]. A hallmark of hypoxic cancer cells is the accumulation of lipid droplets (LD). By inhibiting intracellular lipolysis mediated by adipose triglyceride lipase (ATGL) a small protein encoded by hypoxia-inducible gene 2 HIG2 is one of the major underlying mechanisms. LD accumulation is promoted by hypoxia by inhibiting ATGL-catalyzed lipolysis in solid tumors [52]. When metabolic demand is increased, TA stores in LDs undergo lipolysis to release free FAs. ATGL, hormone-sensitive lipase, and monoacylglycerol lipase are sequentially responsible for whole lipolysis in adipocytes [53-55]. By mediating lipolysis and its protein regulators and converting TG to diacylglycerol and one free FA, ATGL, the rate-limiting intracellular TG hydrolase, catalyzes the initial step in lipolysis [56]. Hence, the gene set enrichment analysis suggested that prognostic model of au-lncRNAs was associated with the TME, including immunotherapy, cancer-related inflammation, and metabolic reprogramming.

Our research has several limitations. First of all, the data in this article are all from the TCGA-PRAD public database. It would be better if

clinical PCa samples can be added for verification. Secondly, although we have conducted in vitro cell experiments, there may be differences in cell lines and tissue samples. Further research is needed to confirm our findings. Finally, we found that the survival rate of PCa in the TCGA data set was as high as 99%, and the prognostic OS index was not available, so the DFS index was used to model the prognosis model. No suitable verification data set was found in other public databases such as ICGC, so finally the TCGA sample was randomly divided into 70% samples as the modeling set and 30% samples as the verification set.

All in all, the overall modeling effect of this study is good. The relationship be-tween au-lncRNA and PCa can be analyzed from multiple angles. Based on five au-lncRNAs, we have developed a model that can anticipate the prognosis of individuals with PCa. We also evaluated the expression levels of 5 lncRNAs in prognostic signatures through qRT-PCR experiments, which further verified our bioinformatics results. Due to the different roles of lncRNAs, these au-lncRNAs might become hopeful targets for the treatment of PCa. The outcomes of this investigation present fresh perspectives for examining prognosis of PCa.

Conclusion

In conclusion, our au-lncRNA prognostic model may be useful in predicting PCa prognosis and has therapeutic applications. These lncRNAs might be crucial in the diagnosis and management of PCa.

Disclosure of conflict of interest

None.

Abbreviations

ATGL, Adipose Triglyceride Lipase; AUC, Area Under Curve; Au-lncRNAs, Autophagy-related lncRNAs; CARs, Chimeric Antigen Receptors; CRPC, Castration Resistance Prostate Cancer; DFS, Disease-Free Survival; GO, Gene Ontology; GS, Gleason Score; GSEA, Gene Set Enrichment Analysis; KEGG, Kyoto Encyclopedia of Genes and Genomes; LD, Lipid Droplet; LncRNAs, Long non-coding RNAs; PCa, Prostate Cancer; PRRs, Pattern Recognition Receptors; PSA, Prostate-Specific Antigen; RAGE, Receptor for Advanced Glycation End-products; RLP, Residual Lipoprotein; ROC, Receiver Operator Characteristic; TCGA, the Cancer Genome Atlas; TLR, Toll-Like Receptor; TME, Tumor Microenvironment.

Address correspondence to: Hong Weng and Shuai Yuan, Center for Evidence-Based and Translational Medicine, Zhongnan Hospital of Wuhan University, Wuhan, Hubei, China. E-mail: wenghong@whu.edu.cn (HW); yuanshuai021@whu.edu.cn (SY)

References

[1] Zi H, He SH, Leng XY, Xu XF, Huang Q, Weng H, Zhu C, Li LY, Gu JM, Li XH, Ming DJ, Li XD, Yuan S, Wang XH, He DL and Zeng XT. Global, regional, and national burden of kidney, bladder, and prostate cancers and their attributable risk factors, 1990-2019. Mil Med Res 2021; 8: 60.

[2] Global Burden of Disease Cancer Collaboration, Fitzmaurice C, Abate D, Abbasi N, Abbastabar H, Abd-Allah F, Abdel-Rahman O, Abdelalim A, Abdoli A, Abdollahpour I, Abdulle ASM, Abebe ND, Abraha HN, Abu-Raddad LJ, Abualhasan A, Adedeji IA, Advani SM, Afarideh M, Afshari M, Aghaali M, Agius D, Agrawal S, Ahmadi A, Ahmadian E, Ahmadpour E, Ahmed MB, Akbari ME, Akinyemiju T, Al-Aly Z, AlAbdulKader AM, Alahdab F, Alam T, Alamene GM, Alemnew BTT, Alene KA, Alinia C, Alipour V, Aljunid SM, Bakeshei FA, Almadi MAH, Almasi-Hashiani A, Alsharif U, Alsowaidi S, Alvis-Guzman N, Amini E, Amini S, Amoako YA, Anbari Z, Anber NH, Andrei CL, Anjomshoa M, Ansari F, Ansariadi A, Appiah SCY, Arab-Zozani M, Arabloo J, Arefi Z, Aremu O, Areri HA, Artaman A, Asayesh H, Asfaw ET, Ashagre AF, Assadi R, Ataeinia B, Atalay HT, Ataro Z, Atique S, Ausloos M, Avila-Burgos L, Avokpaho EFGA, Awasthi A, Awoke N, Ayala Quintanilla BP, Ayanore MA, Ayele HT, Babaee E, Bacha U, Badawi A, Bagherzadeh M, Bagli E, Balakrishnan S, Balouchi A, Bärnighausen TW, Battista RJ, Behzadifar M, Behzadifar M, Bekele BB, Belay YB, Belayneh YM, Berfield KKS, Berhane A, Bernabe E, Beuran M, Bhakta N, Bhattacharyya K, Biadgo B, Bijani A, Bin Sayeed MS, Birungi C, Bisignano C, Bitew H, Bjørge T, Bleyer A, Bogale KA, Bojia HA, Borzì AM, Bosetti C, Bou-Orm IR, Brenner H, Brewer JD, Briko AN, Briko NI, Bustamante-Teixeira MT, Butt ZA, Carreras G, Carrero JJ, Carvalho F, Castro C, Castro F, Catalá-López F, Cerin E, Chaiah Y, Chanie WF, Chattu VK, Chaturvedi P, Chauhan NS, Chehrazi M, Chiang PP, Chichiabellu TY, Chido-Amajuoyi OG, Chimed-Ochir O, Choi JJ, Christopher DJ, Chu DT, Constantin MM, Costa VM, Crocetti E, Crowe CS, Curado MP, Dahlawi SMA, Damiani G, Darwish AH, Daryani A, das Neves J, Deme-

ke FM, Demis AB, Demissie BW, Demoz GT, Denova-Gutiérrez E, Derakhshani A, Deribe KS, Desai R, Desalegn BB, Desta M, Dey S, Dharmaratne SD, Dhimal M, Diaz D, Dinberu MTT, Djalalinia S, Doku DT, Drake TM, Dubey M, Dubljanin E, Duken EE, Ebrahimi H, Effiong A, Eftekhari A, El Sayed I, Zaki MES, El-Jaafary SI, El-Khatib Z, Elemineh DA, Elkout H, Ellenbogen RG, Elsharkawy A, Emamian MH, Endalew DA, Endries AY, Eshrati B, Fadhil I, Fallah Omrani V, Faramarzi M, Farhangi MA, Farioli A, Farzadfar F, Fentahun N, Fernandes E, Feyissa GT, Filip I, Fischer F, Fisher JL, Force LM, Foroutan M, Freitas M, Fukumoto T, Futran ND, Gallus S, Gankpe FG, Gayesa RT, Gebrehiwot TT, Gebremeskel GG, Gedefaw GA, Gelaw BK, Geta B, Getachew S, Gezae KE, Ghafourifard M, Ghajar A, Ghashghaee A, Gholamian A, Gill PS, Ginindza TTG, Girmay A, Gizaw M, Gomez RS, Gopalani SV, Gorini G, Goulart BNG, Grada A, Ribeiro Guerra M, Guimaraes ALS, Gupta PC, Gupta R, Hadkhale K, Haj-Mirzaian A, Haj-Mirzaian A, Hamadeh RR, Hamidi S, Hanfore LK, Haro JM, Hasankhani M, Hasanzadeh A, Hassen HY, Hay RJ, Hay SI, Henok A, Henry NJ, Herteliu C, Hidru HD, Hoang CL, Hole MK, Hoogar P, Horita N, Hosgood HD, Hosseini M, Hosseinzadeh M, Hostiuc M, Hostiuc S, Househ M, Hussen MM, Ileanu B, Ilic MD, Inos K, Irvani SSN, Iseh KR, Islam SMS, Islami F, Jafari Balalami N, Jafarinia M, Jahangiry L, Jahani MA, Jahanmehr N, Jakovljevic M, James SL, Javanbakht M, Jayaraman S, Jee SH, Jenabi E, Jha RP, Jonas JB, Jonnagaddala J, Joo T, Jungari SB, Jürisson M, Kabir A, Kamangar F, Karch A, Karimi N, Karimian A, Kasaeian A, Kasahun GG, Kassa B, Kassa TD, Kassaw MW, Kaul A, Keiyoro PN, Kelbore AG, Kerbo AA, Khader YS, Khalilarjmandi M, Khan EA, Khan G, Khang YH, Khatab K, Khater A, Khayamzadeh M, Khazaee-Pool M, Khazaei S, Khoja AT, Khosravi MH, Khubchandani J, Kianipour N, Kim D, Kim YJ, Kisa A, Kisa S, Kissimova-Skarbek K, Komaki H, Koyanagi A, Krohn KJ, Bicer BK, Kugbey N, Kumar V, Kuupiel D, La Vecchia C, Lad DP, Lake EA, Lakew AM, Lal DK, Lami FH, Lan Q, Lasrado S, Lauriola P, Lazarus JV, Leigh J, Leshargie CT, Liao Y, Limenih MA, Listl S, Lopez AD, Lopukhov PD, Lunevicius R, Madadin M, Magdeldin S, El Razek HMA, Majeed A, Maleki A, Malekzadeh R, Manafi A, Manafi N, Manamo WA, Mansourian M, Mansournia MA, Mantovani LG, Maroufizadeh S, Martini SMS, Mashamba-Thompson TP, Massenburg BB, Maswabi MT, Mathur MR, McAlinden C, McKee M, Meheretu HAA, Mehrotra R, Mehta V, Meier T, Melaku YA, Meles GG, Meles HG, Melese A, Melku M, Memiah PTN, Mendoza W, Menezes RG, Merat S, Meretoja TJ, Mestrovic T, Miazgowski B, Miazgowski T, Mihretie KMM, Miller TR, Mills EJ, Mir SM, Mirzaei H, Mirzaei HR, Mishra R, Moazen B, Mohammad DK, Mohammad KA, Mohammad Y, Darwesh AM, Mohammadbeigi A, Mohammadi H, Mohammadi M, Mohammadian M, Mohammadian-Hafshejani A, Mohammadoo-Khorasani M, Mohammadpourhodki R, Mohammed AS, Mohammed JA, Mohammed S, Mohebi F, Mokdad AH, Monasta L, Moodley Y, Moosazadeh M, Moossavi M, Moradi G, Moradi-Joo M, Moradi-Lakeh M, Moradpour F, Morawska L, Morgado-da-Costa J, Morisaki N, Morrison SD, Mosapour A, Mousavi SM, Muche AA, Muhammed OSS, Musa J, Nabhan AF, Naderi M, Nagarajan AJ, Nagel G, Nahvijou A, Naik G, Najafi F, Naldi L, Nam HS, Nasiri N, Nazari J, Negoi I, Neupane S, Newcomb PA, Nggada HA, Ngunjiri JW, Nguyen CT, Nikniaz L, Ningrum DNA, Nirayo YL, Nixon MR, Nnaji CA, Nojomi M, Nosratnejad S, Shiadeh MN, Obsa MS, Ofori-Asenso R, Ogbo FA, Oh IH, Olagunju AT, Olagunju TO, Oluwasanu MM, Omonisi AE, Onwujekwe OE, Oommen AM, Oren E, Ortega-Altamirano DDV, Ota E, Otstavnov SS, Owolabi MO, P A M, Padubidri JR, Pakhale S, Pakpour AH, Pana A, Park EK, Parsian H, Pashaei T, Patel S, Patil ST, Pennini A, Pereira DM, Piccinelli C, Pillay JD, Pirestani M, Pishgar F, Postma MJ, Pourjafar H, Pourmalek F, Pourshams A, Prakash S, Prasad N, Qorbani M, Rabiee M, Rabiee N, Radfar A, Rafiei A, Rahim F, Rahimi M, Rahman MA, Rajati F, Rana SM, Raoofi S, Rath GK, Rawaf DL, Rawaf S, Reiner RC, Renzaho AMN, Rezaei N, Rezapour A, Ribeiro AI, Ribeiro D, Ronfani L, Roro EM, Roshandel G, Rostami A, Saad RS, Sabbagh P, Sabour S, Saddik B, Safiri S, Sahebkar A, Salahshoor MR, Salehi F, Salem H, Salem MR, Salimzadeh H, Salomon JA, Samy AM, Sanabria J, Santric Milicevic MM, Sartorius B, Sarveazad A, Sathian B, Satpathy M, Savic M, Sawhney M, Sayyah M, Schneider IJC, Schöttker B, Sekerija M, Sepanlou SG, Sepehrimanesh M, Seyedmousavi S, Shaahmadi F, Shabaninejad H, Shahbaz M, Shaikh MA, Shamshirian A, Shamsizadeh M, Sharafi H, Sharafi Z, Sharif M, Sharifi A, Sharifi H, Sharma R, Sheikh A, Shirkoohi R, Shukla SR, Si S, Siabani S, Silva DAS, Silveira DGA, Singh A, Singh JA, Sisay S, Sitas F, Sobngwi E, Soofi M, Soriano JB, Stathopoulou V, Sufiyan MB, Tabarés-Seisdedos R, Tabuchi T, Takahashi K, Tamtaji OR, Tarawneh MR, Tassew SG, Taymoori P, Tehrani-Banihashemi A, Temsah MH, Temsah O, Tesfay BE, Tesfay FH, Teshale MY, Tessema GA, Thapa S, Tlaye KG, Topor-Madry R, Tovani-Palone MR, Traini E, Tran BX, Tran KB, Tsadik AG, Ullah I, Uthman OA, Vacante M, Vaezi M, Varona Pérez P, Veisani Y, Vidale S, Violante FS, Vlassov V, Vollset

SE, Vos T, Vosoughi K, Vu GT, Vujcic IS, Wabinga H, Wachamo TM, Wagnew FS, Waheed Y, Weldegebreal F, Weldesamuel GT, Wijeratne T, Wondafrash DZ, Wonde TE, Wondmieneh AB, Workie HM, Yadav R, Yadegar A, Yadollahpour A, Yaseri M, Yazdi-Feyzabadi V, Yeshaneh A, Yimam MA, Yimer EM, Yisma E, Yonemoto N, Younis MZ, Yousefi B, Yousefifard M, Yu C, Zabeh E, Zadnik V, Moghadam TZ, Zaidi Z, Zamani M, Zandian H, Zangeneh A, Zaki L, Zendehdel K, Zenebe ZM, Zewale TA, Ziapour A, Zodpey S and Murray CJL. Global, regional, and national cancer incidence, mortality, years of life lost, years lived with disability, and disability-adjusted life-years for 29 cancer groups, 1990 to 2017: a systematic analysis for the global burden of disease study. JAMA Oncol 2019; 5: 1749-1768.

[3] Chandra Gupta S and Nandan Tripathi Y. Potential of long non-coding RNAs in cancer patients: from biomarkers to therapeutic targets. Int J Cancer 2017; 140: 1955-1967.

[4] Mitra SA, Mitra AP and Triche TJ. A central role for long non-coding RNA in cancer. Front Genet 2012; 3: 17.

[5] Guttman M, Donaghey J, Carey BW, Garber M, Grenier JK, Munson G, Young G, Lucas AB, Ach R, Bruhn L, Yang X, Amit I, Meissner A, Regev A, Rinn JL, Root DE and Lander ES. lincRNAs act in the circuitry controlling pluripotency and differentiation. Nature 2011; 477: 295-300.

[6] Yuan P, Cao W, Zang Q, Li G, Guo X and Fan J. The HIF-2α-MALAT1-miR-216b axis regulates multi-drug resistance of hepatocellular carcinoma cells via modulating autophagy. Biochem Biophys Res Commun 2016; 478: 1067-1073.

[7] Xue C, Chen C, Gu X and Li L. Progress and assessment of lncRNA DGCR5 in malignant phenotype and immune infiltration of human cancers. Am J Cancer Res 2021; 11: 1-13.

[8] Du Z, Fei T, Verhaak RG, Su Z, Zhang Y, Brown M, Chen Y and Liu XS. Integrative genomic analyses reveal clinically relevant long noncoding RNAs in human cancer. Nat Struct Mol Biol 2013; 20: 908-913.

[9] Prensner JR, Iyer MK, Balbin OA, Dhanasekaran SM, Cao Q, Brenner JC, Laxman B, Asangani IA, Grasso CS, Kominsky HD, Cao X, Jing X, Wang X, Siddiqui J, Wei JT, Robinson D, Iyer HK, Palanisamy N, Maher CA and Chinnaiyan AM. Transcriptome sequencing across a prostate cancer cohort identifies PCAT-1, an unannotated lincRNA implicated in disease progression. Nat Biotechnol 2011; 29: 742-749.

[10] Guo H, Ahmed M, Zhang F, Yao CQ, Li S, Liang Y, Hua J, Soares F, Sun Y, Langstein J, Li Y, Poon C, Bailey SD, Desai K, Fei T, Li Q, Sendorek DH, Fraser M, Prensner JR, Pugh TJ, Pomerantz M, Bristow RG, Lupien M, Feng FY, Boutros PC, Freedman ML, Walsh MJ and He HH. Modulation of long noncoding RNAs by risk SNPs underlying genetic predispositions to prostate cancer. Nat Genet 2016; 48: 1142-1150.

[11] Hua JT, Chen S and He HH. Landscape of noncoding RNA in prostate cancer. Trends Genet 2019; 35: 840-851.

[12] Sun T. Long noncoding RNAs act as regulators of autophagy in cancer. Pharmacol Res 2018; 129: 151-155.

[13] Galluzzi L, Pietrocola F, Bravo-San Pedro JM, Amaravadi RK, Baehrecke EH, Cecconi F, Codogno P, Debnath J, Gewirtz DA, Karantza V, Kimmelman A, Kumar S, Levine B, Maiuri MC, Martin SJ, Penninger J, Piacentini M, Rubinsztein DC, Simon HU, Simonsen A, Thorburn AM, Velasco G, Ryan KM and Kroemer G. Autophagy in malignant transformation and cancer progression. EMBO J 2015; 34: 856-880.

[14] Chinnapaka S, Bakthavachalam V and Munirathinam G. Repurposing antidepressant sertraline as a pharmacological drug to target prostate cancer stem cells: dual activation of apoptosis and autophagy signaling by deregulating redox balance. Am J Cancer Res 2020; 10: 2043-2065.

[15] Bennett HL, Stockley J, Fleming JT, Mandal R, O'Prey J, Ryan KM, Robson CN and Leung HY. Does androgen-ablation therapy (AAT) associated autophagy have a pro-survival effect in LNCaP human prostate cancer cells? BJU Int 2013; 111: 672-682.

[16] Jia J, Zhang HB, Shi Q, Yang C, Ma JB, Jin B, Wang X, He D and Guo P. KLF5 downregulation desensitizes castration-resistant prostate cancer cells to docetaxel by increasing BECN1 expression and inducing cell autophagy. Theranostics 2019; 9: 5464-5477.

[17] Katheder NS, Khezri R, O'Farrell F, Schultz SW, Jain A, Rahman MM, Schink KO, Theodossiou TA, Johansen T, Juhász G, Bilder D, Brech A, Stenmark H and Rusten TE. Microenvironmental autophagy promotes tumour growth. Nature 2017; 541: 417-420.

[18] Tzanakakis G, Giatagana EM, Kuskov A, Berdiaki A, Tsatsakis AM, Neagu M and Nikitovic D. Proteoglycans in the pathogenesis of hormone-dependent cancers: mediators and effectors. Cancers (Basel) 2020; 12: 2401.

[19] Ma X, Zou L, Li X, Chen Z, Lin Z and Wu X. Inhibition of autophagy improves the efficacy of abiraterone for the treatment of prostate cancer. Cancer Biother Radiopharm 2019; 34: 181-188.

[20] Kaini RR, Sillerud LO, Zhaorigetu S and Hu CA. Autophagy regulates lipolysis and cell survival through lipid droplet degradation in androgen-

sensitive prostate cancer cells. Prostate 2012; 72: 1412-1422.
[21] Jemal A, Ma J, Siegel R, Fedewa S, Brawley O and Ward EM. Prostate cancer incidence rates 2 years after the US preventive services task force recommendations against screening. JAMA Oncol 2016; 2: 1657-1660.
[22] Han M, Partin AW, Zahurak M, Piantadosi S, Epstein JI and Walsh PC. Biochemical (prostate specific antigen) recurrence probability following radical prostatectomy for clinically localized prostate cancer. J Urol 2003; 169: 517-523.
[23] Catalona WJ and Smith DS. 5-year tumor recurrence rates after anatomical radical retropubic prostatectomy for prostate cancer. J Urol 1994; 152: 1837-1842.
[24] Li J, Du H, Chen W, Qiu M, He P and Ma Z. Identification of potential autophagy-associated lncRNA in prostate cancer. Aging (Albany NY) 2021; 13: 13153-13165.
[25] Chen G, Qin X, Wang Y, Gao B, Ling M, Yin W, Li Y and Pan B. Expression status and prognostic value of autophagy-related lncRNAs in prostate cancer. Cell Cycle 2022; 21: 1684-1696.
[26] Ge H, Yan Y, Wu D, Huang Y and Tian F. Potential role of LINC00996 in colorectal cancer: a study based on data mining and bioinformatics. Onco Targets Ther 2018; 11: 4845-4855.
[27] Zhou S, Fang J, Sun Y and Li H. Integrated analysis of a risk score system predicting prognosis and a ceRNA network for differentially expressed lncRNAs in multiple myeloma. Front Genet 2020; 11: 934.
[28] Lina S. Identification of hub lncRNAs in head and neck cancer based on weighted gene co-expression network analysis and experiments. FEBS Open Bio 2021; 11: 2060-2073.
[29] Guo J and Pan H. Long noncoding RNA LINC01125 enhances cisplatin sensitivity of ovarian cancer via miR-1972. Med Sci Monit 2019; 25: 9844-9854.
[30] Wan W, Hou Y, Wang K, Cheng Y, Pu X and Ye X. The LXR-623-induced long non-coding RNA LINC01125 suppresses the proliferation of breast cancer cells via PTEN/AKT/p53 signaling pathway. Cell Death Dis 2019; 10: 248.
[31] Li N and Zhan X. Identification of clinical trait-related lncRNA and mRNA biomarkers with weighted gene co-expression network analysis as useful tool for personalized medicine in ovarian cancer. EPMA J 2019; 10: 273-290.
[32] Shen Y, Li N, Wu S, Zhou Y, Shan Y, Zhang Q, Ding C, Yuan Q, Zhao F, Zeng R and Zhu X. Nudel binds Cdc42GAP to modulate Cdc42 activity at the leading edge of migrating cells. Dev Cell 2008; 14: 342-353.
[33] Sekine Y, Koike H, Nakano T, Nakajima K and Suzuki K. Remnant lipoproteins stimulate proliferation and activate MAPK and Akt signaling pathways via G protein-coupled receptor in PC-3 prostate cancer cells. Clin Chim Acta 2007; 383: 78-84.
[34] Sfanos KS and De Marzo AM. Prostate cancer and inflammation: the evidence. Histopathology 2012; 60: 199-215.
[35] Hood SP, Foulds GA, Imrie H, Reeder S, McArdle SEB, Khan M and Pockley AG. Phenotype and function of activated natural killer cells from patients with prostate cancer: patient-dependent responses to priming and IL-2 activation. Front Immunol 2018; 9: 3169.
[36] Liu Q, Russell MR, Shahriari K, Jernigan DL, Lioni MI, Garcia FU and Fatatis A. Interleukin-1β promotes skeletal colonization and progression of metastatic prostate cancer cells with neuroendocrine features. Cancer Res 2013; 73: 3297-3305.
[37] Garcia AJ, Ruscetti M, Arenzana TL, Tran LM, Bianci-Frias D, Sybert E, Priceman SJ, Wu L, Nelson PS, Smale ST and Wu H. Pten null prostate epithelium promotes localized myeloid-derived suppressor cell expansion and immune suppression during tumor initiation and progression. Mol Cell Biol 2014; 34: 2017-2028.
[38] Zhunussova A, Sen B, Friedman L, Tuleukhanov S, Brooks AD, Sensenig R and Orynbayeva Z. Tumor microenvironment promotes dicarboxylic acid carrier-mediated transport of succinate to fuel prostate cancer mitochondria. Am J Cancer Res 2015; 5: 1665-1679.
[39] Kasahara Y, Shirota H, Umegaki S and Ishioka C. Contribution of Fcγ receptor IIB to creating a suppressive tumor microenvironment in a mouse model. Cancer Immunol Immunother 2019; 68: 1769-1778.
[40] Chiaruttini G, Mele S, Opzoomer J, Crescioli S, Ilieva KM, Lacy KE and Karagiannis SN. B cells and the humoral response in melanoma: the overlooked players of the tumor microenvironment. Oncoimmunology 2017; 6: e1294296.
[41] Russell BL, Sooklal SA, Malindisa ST, Daka LJ and Ntwasa M. The tumor microenvironment factors that promote resistance to immune checkpoint blockade therapy. Front Oncol 2021; 11: 641428.
[42] Razeghian E, Nasution MKM, Rahman HS, Gardanova ZR, Abdelbasset WK, Aravindhan S, Bokov DO, Suksatan W, Nakhaei P, Shariatzadeh S, Marofi F, Yazdanifar M, Shamlou S, Motavalli R and Khiavi FM. A deep insight into CRISPR/Cas9 application in CAR-T cell-based tumor immunotherapies. Stem Cell Res Ther 2021; 12: 428.
[43] de Sousa E, Lérias JR, Beltran A, Paraschoudi G, Condeço C, Kamiki J, António PA, Figueiredo N, Carvalho C, Castillo-Martin M, Wang Z,

Ligeiro D, Rao M and Maeurer M. Targeting neoepitopes to treat solid malignancies: immunosurgery. Front Immunol 2021; 12: 592031.
[44] Hangai S, Kimura Y, Taniguchi T and Yanai H. Signal-transducing innate receptors in tumor immunity. Cancer Sci 2021; 112: 2578-2591.
[45] Azizian-Farsani F, Abedpoor N, Hasan Sheikhha M, Gure AO, Nasr-Esfahani MH and Ghaedi K. Receptor for advanced glycation end products acts as a fuel to colorectal cancer development. Front Oncol 2020; 10: 552283.
[46] Yuan S, Fang C, Leng WD, Wu L, Li BH, Wang XH, Hu H and Zeng XT. Oral microbiota in the oral-genitourinary axis: identifying periodontitis as a potential risk of genitourinary cancers. Mil Med Res 2021; 8: 54.
[47] Bourquin C, Pommier A and Hotz C. Harnessing the immune system to fight cancer with Toll-like receptor and RIG-I-like receptor agonists. Pharmacol Res 2020; 154: 104192.
[48] Bourquin C, Schmidt L, Hornung V, Wurzenberger C, Anz D, Sandholzer N, Schreiber S, Voelkl A, Hartmann G and Endres S. Immunostimulatory RNA oligonucleotides trigger an antigen-specific cytotoxic T-cell and IgG2a response. Blood 2007; 109: 2953-2960.
[49] Wang J, Boddupalli A, Koelbl J, Nam DH, Ge X, Bratlie KM and Schneider IC. Degradation and remodeling of epitaxially grown collagen fibrils. Cell Mol Bioeng 2019; 12: 69-84.
[50] Natividad RJ, Lalli ML, Muthuswamy SK and Asthagiri AR. Golgi stabilization, not its front-rear bias, is associated with EMT-enhanced fibrillar migration. Biophys J 2018; 115: 2067-2077.
[51] Uchugonova A, Zhao M, Weinigel M, Zhang Y, Bouvet M, Hoffman RM and König K. Multiphoton tomography visualizes collagen fibers in the tumor microenvironment that maintain cancer-cell anchorage and shape. J Cell Biochem 2013; 114: 99-102.
[52] Povero D, Johnson SM and Liu J. Hypoxia, hypoxia-inducible gene 2 (HIG2)/HILPDA, and intracellular lipolysis in cancer. Cancer Lett 2020; 493: 71-79.
[53] Zimmermann R, Strauss JG, Haemmerle G, Schoiswohl G, Birner-Gruenberger R, Riederer M, Lass A, Neuberger G, Eisenhaber F, Hermetter A and Zechner R. Fat mobilization in adipose tissue is promoted by adipose triglyceride lipase. Science 2004; 306: 1383-1386.
[54] Zechner R, Zimmermann R, Eichmann TO, Kohlwein SD, Haemmerle G, Lass A and Madeo F. FAT SIGNALS-lipases and lipolysis in lipid metabolism and signaling. Cell Metab 2012; 15: 279-291.
[55] Bezaire V, Mairal A, Ribet C, Lefort C, Girousse A, Jocken J, Laurencikiene J, Anesia R, Rodriguez AM, Ryden M, Stenson BM, Dani C, Ailhaud G, Arner P and Langin D. Contribution of adipose triglyceride lipase and hormone-sensitive lipase to lipolysis in hMADS adipocytes. J Biol Chem 2009; 284: 18282-18291.
[56] Lass A, Zimmermann R, Oberer M and Zechner R. Lipolysis - a highly regulated multi-enzyme complex mediates the catabolism of cellular fat stores. Prog Lipid Res 2011; 50: 14-27.

Table S1. The sequences of forward and reverse primers of the 5 autophagy lncRNAs

LncRNA	Primers
LINC01125-F	TTCTCCATCTGCGCACCACA
LINC01125-R	GCCAGCCATCGGTGCCATAT
LINC01547-F	AGGCCAAGAGACAACAGCGATTAC
LINC01547-R	GCCAAGTGTGGACTCAGAGCTTC
LINC00996-F	TGGTTCTGTGCCTTCTGGAC
LINC00996-R	CTGAAGCGAATGAAGCCGTG
AC068580.6-F	CCAAAACCAAACTCCTGCCTG
AC068580.6-R	CGGGTGACCACTTCTTAGGAC
AF131215.2-F	AGCCTGGTGGGTTTACTGTG
AF131215.2-R	TGAACTGCACCGCAACTCTA

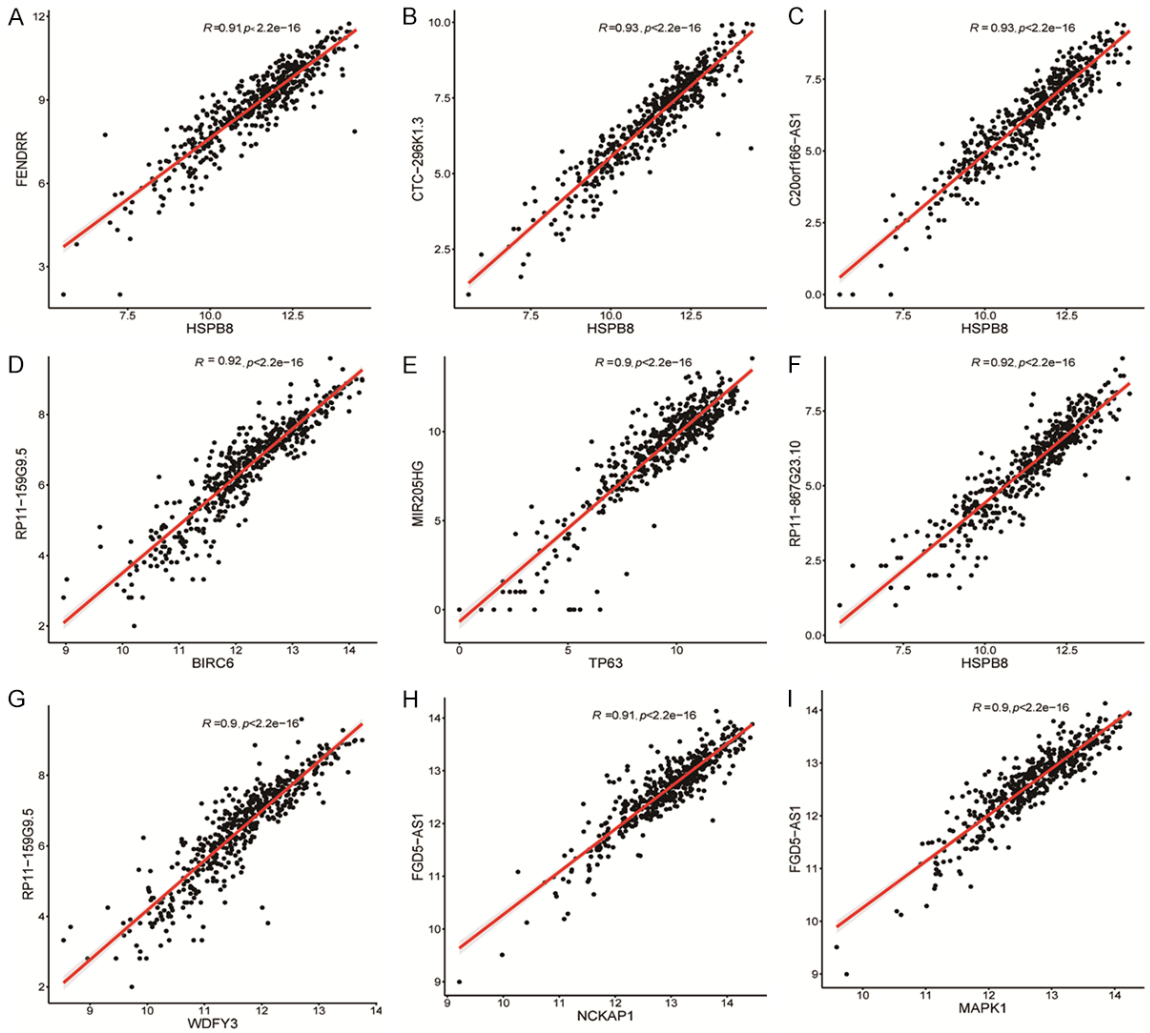

Figure S1. Representative correlation scatter plots of autophagy-related genes and lncRNAs by Pearson correlation analysis (|R| > 0.9, P < 0.05).

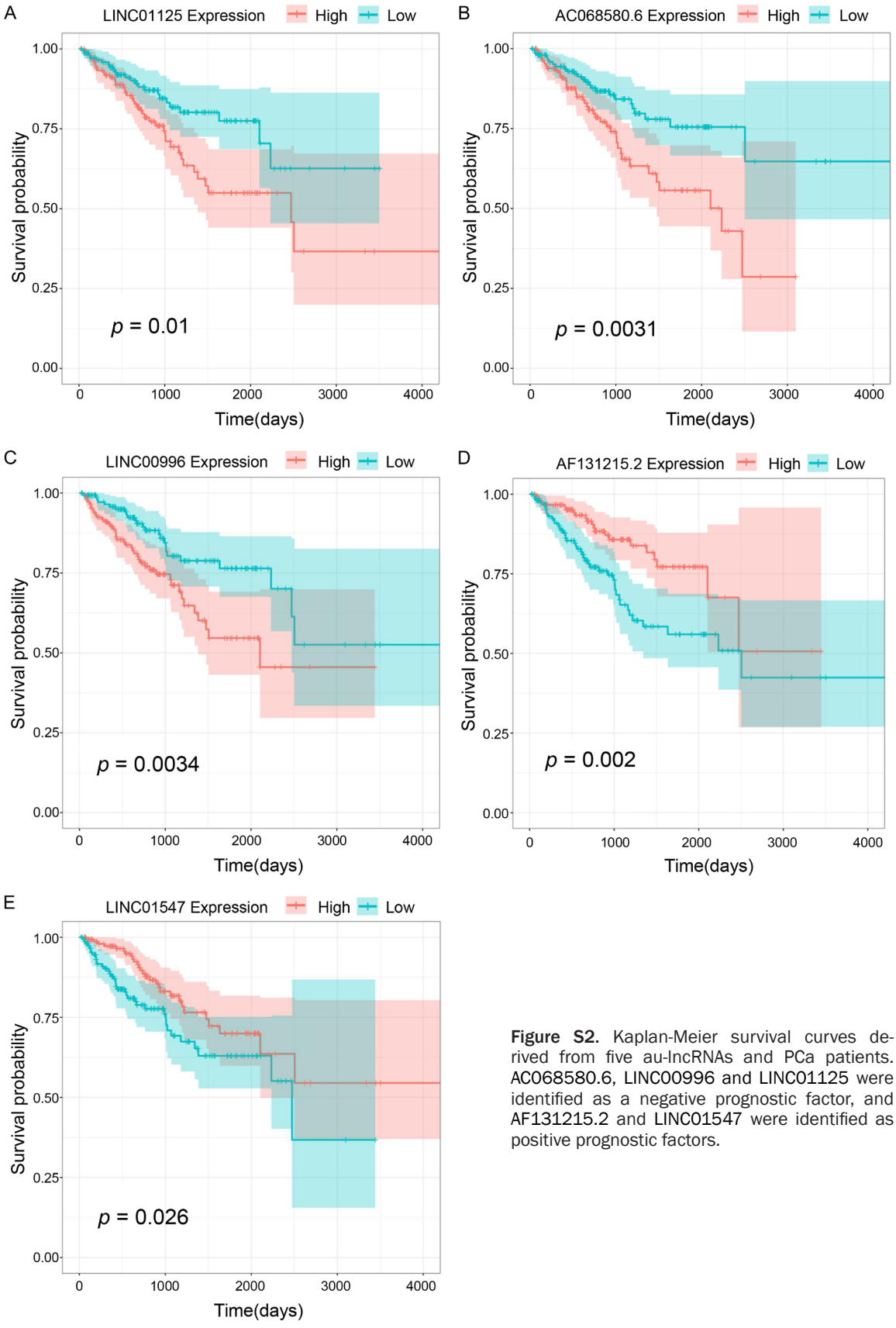

Figure S2. Kaplan-Meier survival curves derived from five au-lncRNAs and PCa patients. AC068580.6, LINC00996 and LINC01125 were identified as a negative prognostic factor, and AF131215.2 and LINC01547 were identified as positive prognostic factors.

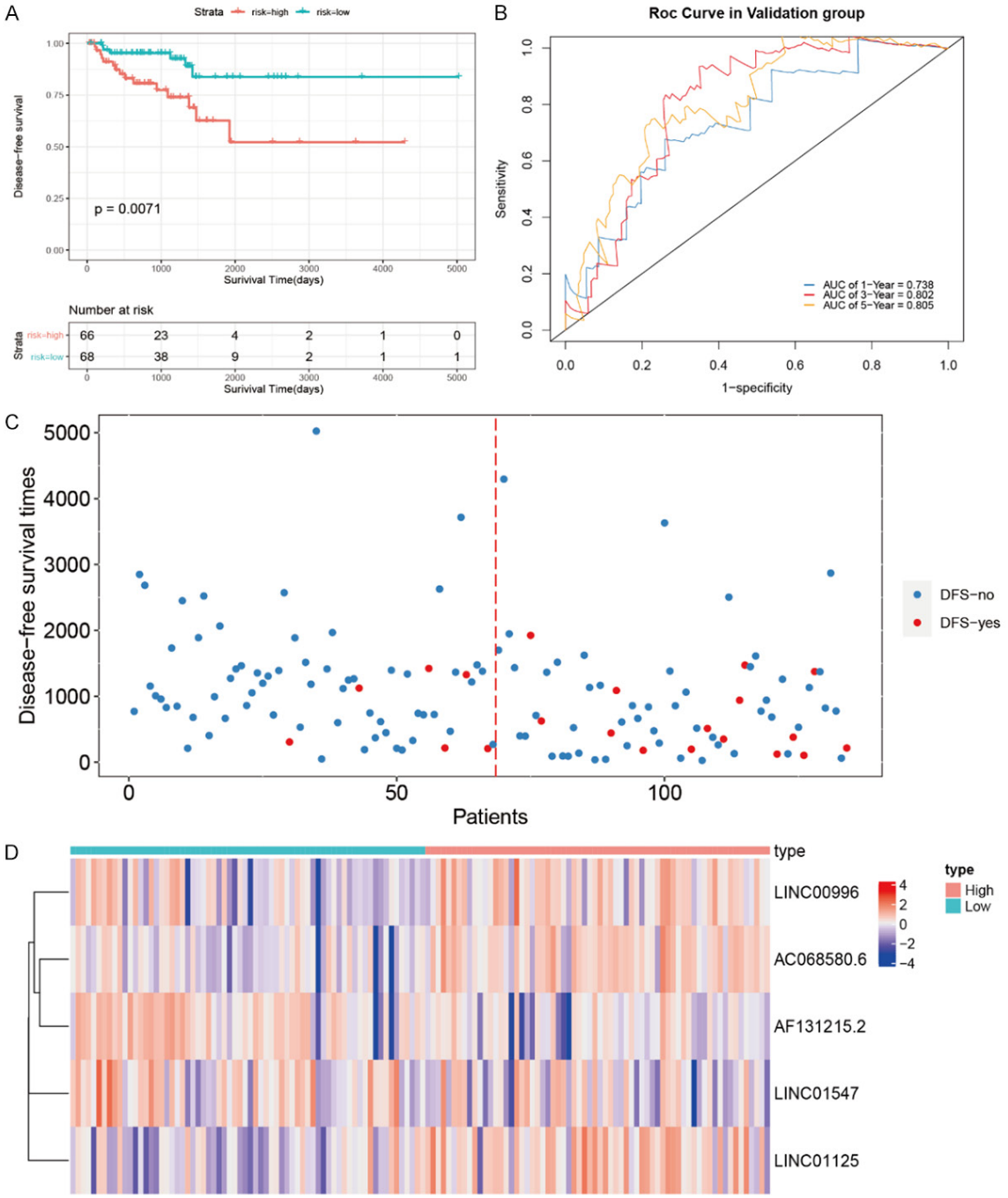

Figure S3. Evaluation of au-lncRNA prognosis model validation set for PCa patients. A. Kaplan-Meier survival curves of the high-risk group and the low-risk group. B. ROC curve based on risk scoring model. C. Scatter plot of the survival situation of the high-risk group and the low-risk group. D. The expression heat map of five autophagy-related lncRNAs.

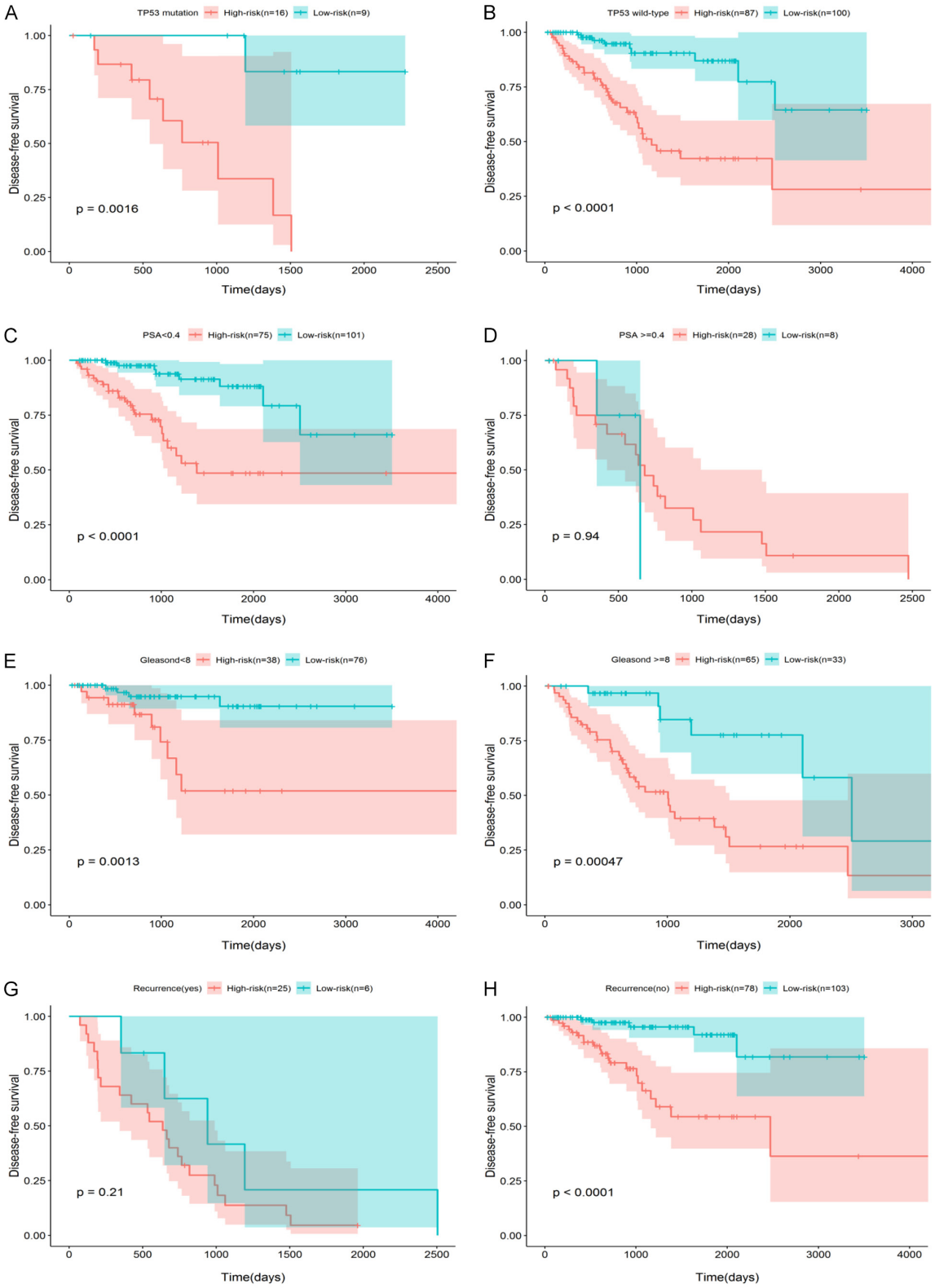
A
TP53 mutation High-risk(n=16) Low-risk(n=9)
Disease-free survival
p = 0.0016
Time(days)
B
TP53 wild-type High-risk(n=87) Low-risk(n=100)
Disease-free survival
p < 0.0001
Time(days)
C
PSA<0.4 High-risk(n=75) Low-risk(n=101)
Disease-free survival
p < 0.0001
Time(days)
D
PSA >=0.4 High-risk(n=28) Low-risk(n=8)
Disease-free survival
p = 0.94
Time(days)
E
Gleasond<8 High-risk(n=38) Low-risk(n=76)
Disease-free survival
p = 0.0013
Time(days)
F
Gleasond >=8 High-risk(n=65) Low-risk(n=33)
Disease-free survival
p = 0.00047
Time(days)
G
Recurrence(yes) High-risk(n=25) Low-risk(n=6)
Disease-free survival
p = 0.21
Time(days)
H
Recurrence(no) High-risk(n=78) Low-risk(n=103)
Disease-free survival
p < 0.0001
Time(days)

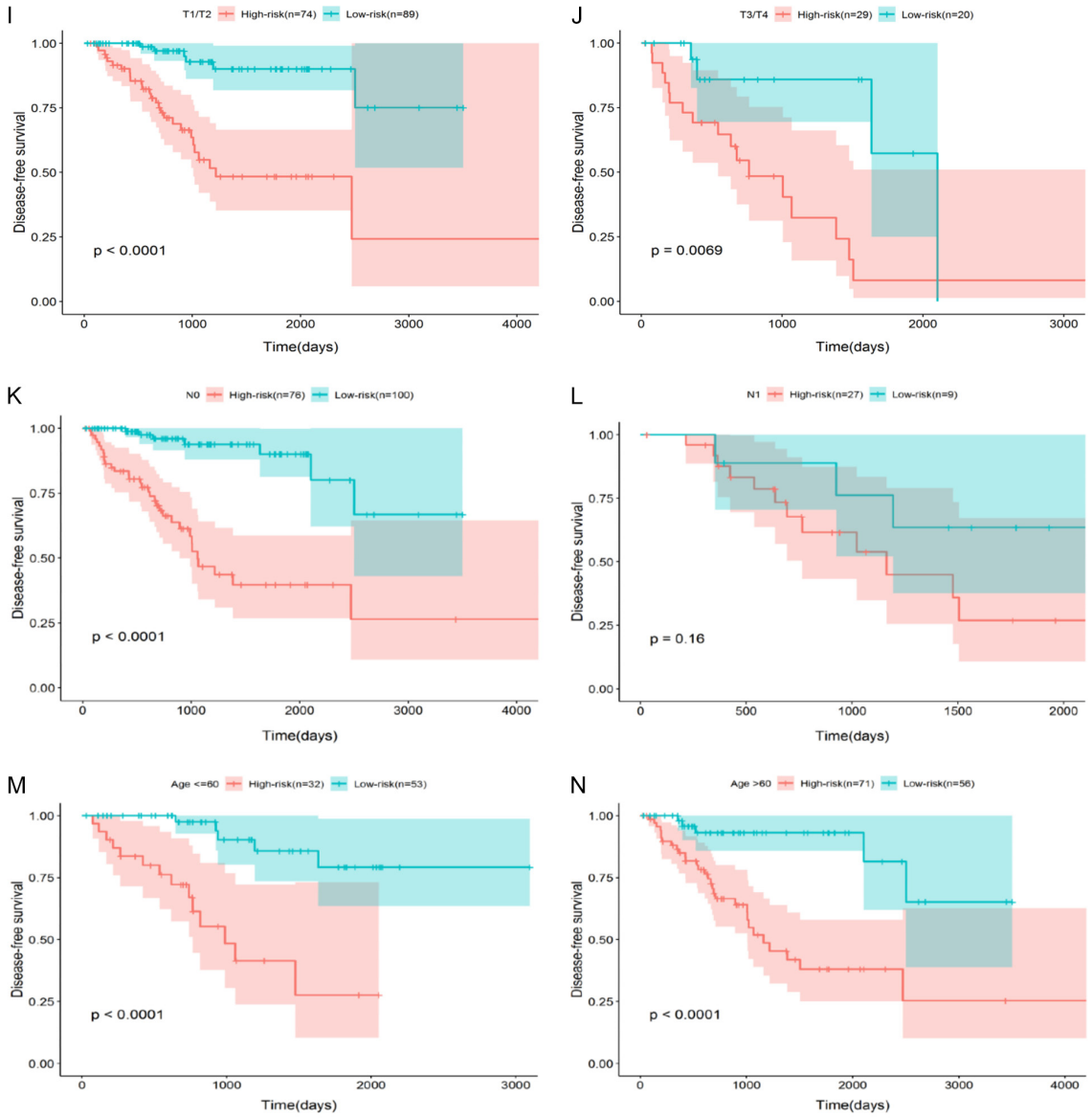

Figure S4. The Kaplan-Meier diagram shows the prediction of DFS time in different clinical subgroups by the prognostic model of au-lncRNAs. A, B. TP53 (mutant and wild type). C, D. PSA (< 4.0 ng/ml and ≥ 4.0 ng/ml). E, F. Gleasond score (< 8 and ≥ 8). G, H. Relapse (yes and no). I, J. T grades (T1/T2 and T3/T4). K, L. N grades (N0 and N1). M, N. Age (≤ 60 and > 60).